Available online at www.sciencedirect.com

ScienceDirect

Journal of Nuclear Materials 363–365 (2007) 325–329

journal of nuclear materials

www.elsevier.com/locate/jnucmat

Analysis of difference in Hα spectral line profiles between attachment and detachment plasmas in LHD

H. Arimoto [a,*], K. Kondo [a], S. Masuzaki [b], M. Shoji [b], J. Miyazawa [b], M. Kobayashi [b], N. Tamura [b], T. Morisaki [b], M. Goto [b], S. Morita [b], K. Ida [b], N. Ohyabu [b], S. Sudo [b] and the LHD Experimental Group[b]

[a] *Graduate School of Energy Science, Kyoto University, Gokasho, Uji, Kyoto 611-0011, Japan*
[b] *National Institute for Fusion Science, 322-6 Oroshi-cho, Toki, Gifu 509-5292, Japan*

Abstract

The sustainable detachment has been achieved in LHD. The line-averaged electron density of the detachment plasmas is typically over 1.0×10^{20} m^{-3}. The difference in the broad component of the Hα spectral line profiles between the attachment and detachment plasmas has been observed. In attachment, the divertor flux much affects the neutral hydrogen generation and the large inward flow up to 1.5×10^4 m/s seemed to be due to the reflection is observed. In detachment, the much smaller flow velocity along the sight lines and the lower Doppler temperature are observed. These observations represent the drastic reduction of the divertor flux and the decrease of the edge electron temperature involved with detachment.

---

1. Introduction

The detachment operation is prospected as an effective method in the fusion devices to reduce the particle and heat load onto the divertor. In JET, the DoD (Degree of Detachment) has been defined and the detachment plasmas in various discharge conditions have been reviewed [1]. The volume recombination in the low temperature regions has been studied in Alcator C-Mod [2], ASDEX-Upgrade [3], DIII-D [4] and W7-AS [6]. The importance of the H_2 molecule behavior has been pointed out by comparing the Fulcher lines and the Balmer series spectra in the attached divertor plasmas with those in the detached plasmas in JT-60U [5]. The characterization of the relations between the neutral hydrogen behavior and the divertor flux, the edge electron temperature is thought to be a key issue.

The sustainable detachment has been achieved in LHD [7]. During detachment, the significant changes in the hydrogen recycling process will be expected. In this paper, we introduce the initial results of the Hα spectral line profile measurements in the attachment and detachment plasmas in LHD. The differences in the neutral hydrogen behavior in such two disparate conditions are discussed, with the profits of the three-dimensional neutral particle transport simulation.

---

[*] Corresponding author. Fax: +81 774 32 9397.
E-mail address: arimoto@center.iae.kyoto-u.ac.jp (H. Arimoto).

0022-3115/$ - see front matter © 2007 Elsevier B.V. All rights reserved.
doi:10.1016/j.jnucmat.2007.01.052

2. Experimental setup

LHD [8] is a superconducting magnetic confinement device with a poloidal/toroidal mode number $l = 2/m = 10$ heliotron configuration, and has the intrinsic divertor structure. The Hα emissions in the inner edge/divertor regions have been observed by an echelle grating spectrometer. Fig. 1 shows schematic overviews of the measurement. A two-dimensional optical fiber array with 30 fibers (3 in the toroidal × 10 in the poloidal directions) has been adopted. The sight line arrangements on the poloidal/toroidal cross-sections are shown in Fig. 1(a) and (b). Each sight line is designated by the column (toroidal direction) and row (poloidal direction) numbers in the fiber array. The emissions are detected by a 1024 × 512 CCD camera. The pixel size of the CCD is 24 μm square and the reciprocal linear dispersion is 0.0024 nm/pixel [9]. The simultaneous acquisition of seven spectra can be made with the minimum time resolution of 200 ms. The spot positions of the sight lines are shown in Fig. 1(c). The sight lines #3–5 to #3–8 view the divertor plates. The diameter of the spots is about 50 mm and the distance between the adjacent spot is about 65 mm. The particle flux to the divertor plate is measured by a Langmuir probe at the divertor plate toroidally equivalent to the the spectroscopy.

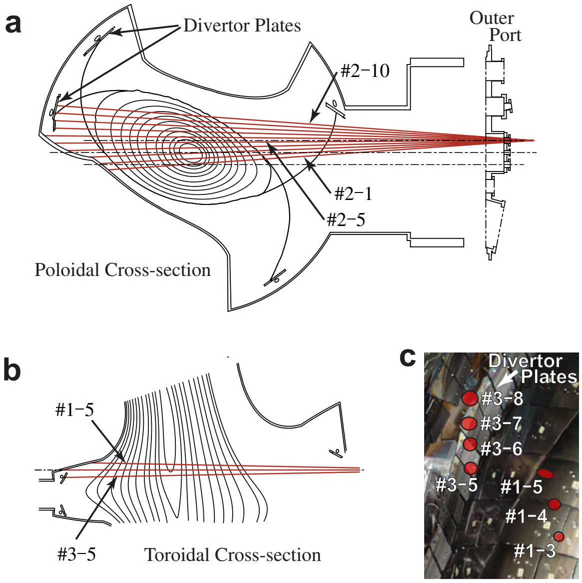

Fig. 1. The schematic overviews of the measurement. The sight line arrangements on the (a) poloidal and (b) toroidal cross-sections and (c) the spot positions of the sight lines on the inner divertor plates and the wall of the vacuum vessel closing to the divertor region.

3. Calculation of neutral hydrogen distributions

The neutral hydrogen density distributions in attachment and detachment have been simulated by the EIRENE code [10]. The experimental data of the (a) electron density and (b) temperature profiles shown in Fig. 2 are used as the input parameters for the simulation. These profiles have been obtained in attachment (rectangles) and detachment (circles) phases of the identical discharge. The plasma column shrinks to $\rho \sim 0.9$ in detachment and the electron density in the core region is much higher than that of attachment. In the simulation, the neutral particle sources are localized at the divertor plates according to the particle flux distributions evaluated by the field line trace. The energy of the reflected atoms and desorbed molecules are determined by the TRIM code [11].

4. Results and discussion

Fig. 3 shows the Hα spectral line profiles measured in the (a) attachment and (b) detachment discharges at the sight line #3–7. These observed line profiles can be decomposed into two Gaussian components of a narrow shape and a broad shape. The narrow component is considered to be the contribution of the emissions from the dissociated atoms and the broad component represents the reflected and charge-exchanged atoms [12,13]. In attachment, the center of the broad component

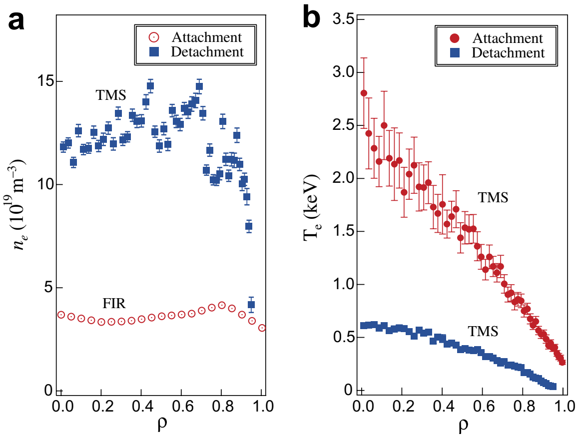

Fig. 2. The (a) n_e and (b) T_e profiles in the attachment and detachment phases in the identical discharge.

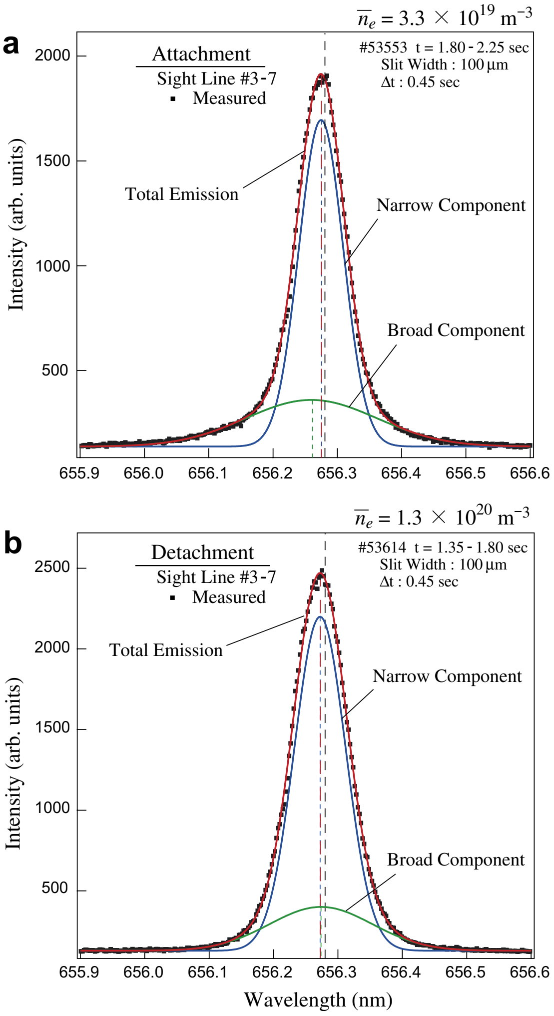

Fig. 3. The Hα spectral line profiles obtained at the sight line #3–7 in the (a) attachment and (b) detachment discharges.

shows the significant blue shift and the line profiles appear to be asymmetric. In the case of Fig. 3(a), the shift of the central wavelength and the FWHM of the broad component correspond to the inward flow velocity of 9.5×10^3 m/s along the sight line and the temperature of the emission atoms of 22.7 eV, respectively. In detachment, the shift of the center of the broad component is much smaller. In the case of Fig. 3(b), the inward flow and the temperature of the broad component are 22.5 m/s and 13.8 eV, respectively. The influence of the emissions from the rotating radiation belt appeared during detachment [14] is not taken into account.

Fig. 4 shows the $\bar{n}_e$ dependences of the line intensity, flow velocity and temperature of the hydrogen atoms, at the sight line #3–6. The filled and open

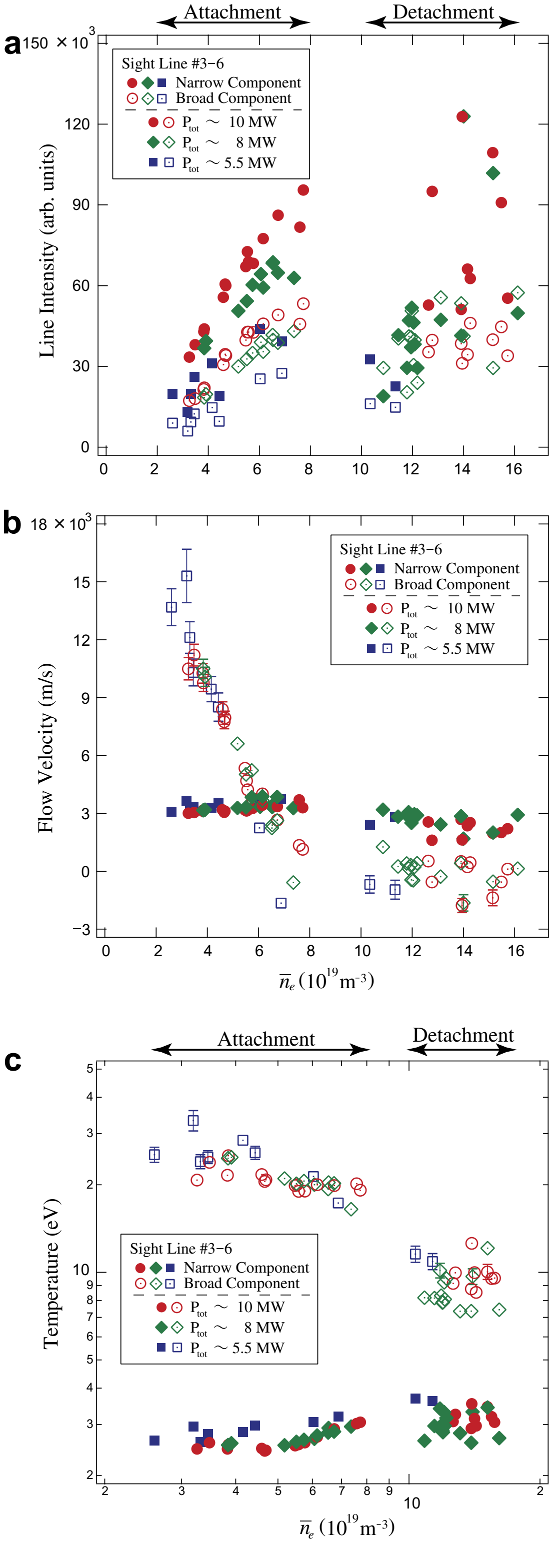

Fig. 4. The $\bar{n}_e$ dependences of (a) the line intensity, (b) the flow velocity along the sight line and (c) the temperature of the emission atoms.

symbols indicate the narrow and broad component, respectively. The symbols are also assorted by the shapes corresponding to the total NB injection power. Fig. 5 shows the $\bar{n}_e$ dependences of the ion saturation current and T_e at $\rho = 0.9$. The $\bar{n}_e$ ranges of $2.6 \leqslant \bar{n}_e \leqslant 7.7 \times 10^{19}\ \mathrm{m}^{-3}$ and $1.0 \leqslant \bar{n}_e \leqslant 1.6 \times 10^{20}\ \mathrm{m}^{-3}$ are correspond to the attachment and detachment regimes. As shown in Fig. 4(a), the line intensities of both components are almost proportional to $\bar{n}_e$ in attachment. A similar dependence is found in the ion saturation current in Fig. 5(a). This means a clear correlation between the neutral hydrogen generation and the divertor flux in attachment. While in detachment, the line intensities are independent of the divertor flux and tend to increase in the higher $\bar{n}_e$ conditions.

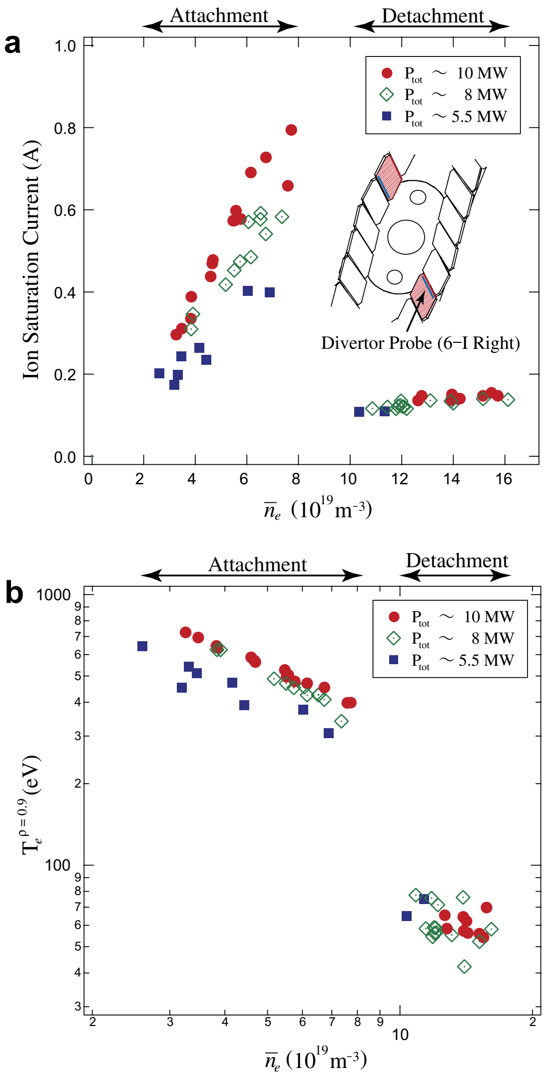

Fig. 5. The $\bar{n}_e$ dependences of (a) the ion saturation current measured by the divertor probe (in the figure) and (b) the electron temperature at $\rho = 0.9$ measured by the Thomson scattering system.

Fig. 6 shows the simulated distributions of the hydrogen atoms and molecules in the (a) attachment and (b) detachment conditions mentioned in Section 2. The sight lines #3–5 to #3–8 are on the cross-section in the figure. In attachment, the hydrogen atoms and molecules are distributed in the vicinity of the divertor region. In detachment, the molecules penetrate inward deeper than in attachment and the atoms are distributed around the inboard ergodic layer and LCFS. These results suggest that the generation processes of the broad component in detachment are different from those in attachment and the emission region is shifted inward.

As shown in Fig. 4(b) and (c), the flow velocity and the temperature of the narrow component do not depend on $\bar{n}_e$, and take almost constant value of $\sim 3.0 \times 10^3$ m/s and ~ 3 eV, respectively, regardless whether attachment or detachment. Those parameters of the broad component in attachment strongly depend on $\bar{n}_e$. The flow velocity drops from $\sim 1.5 \times 10^4$ m/s to ~ 0 m/s with the increase of $\bar{n}_e$. The broad component in this condition is considered to be mainly the reflected atoms by the divertor plates. The drop of the flow velocity with $\bar{n}_e$ can be partly attributed to the decrease of the sheath potential and the energy of the incident ions due to the decrease of the edge electron temperature. The temperature of the atoms is considered to be also affected by the edge electron temperature. In detachment, the contributions of the reflection are scarce because of the drastic decrease of the divertor flux. The flow velocity and the temperature are seemed not to depend on $\bar{n}_e$. The flow along the sight line can be regarded as almost isotropic with a little data scattering and the temperature ranges from about 7 eV to about 13 eV. The broad component in detachment could be qualitatively ascribed to the emissions from the charge-exchanged atoms.

5. Summary

The differences in the neutral hydrogen behavior between attachment and detachment are discussed. In attachment, the divertor flux much affects the neutral hydrogen generation. The blue shift of the broad component can be ascribed to the reflected atoms by the divertor plates. On the other hand, the influence of the divertor flux is scarcely observed

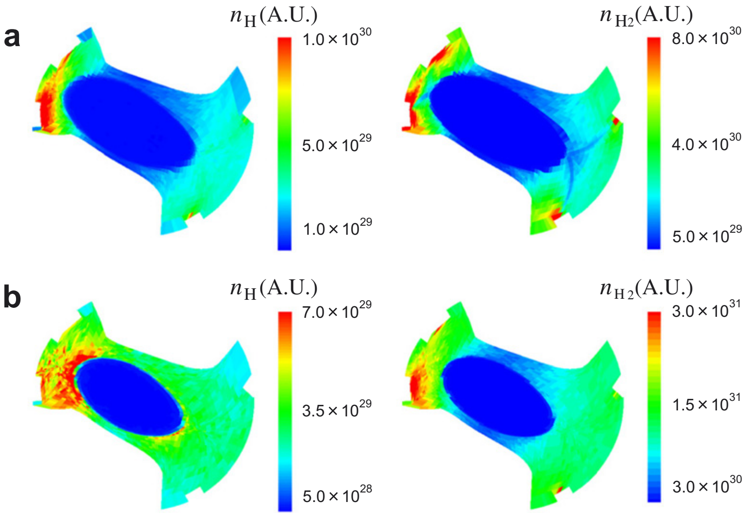

Fig. 6. The simulated hydrogen atoms/molecules distributions in the (a) attachment and (b) detachment conditions. The poloidal cross-section in the figure includes the sight lines #3–5 to #3–8.

in detachment. The generation processes of the broad component in detachment are different from those in attachment and the emission region is shifted inward. The charge-exchanged atoms around the shrunk core plasma may contribute to the broad component in detachment. The difference in the broad component between attachment and detachment can be attributed to the significant differences in the divertor flux and the edge electron temperature. Further investigation is needed to evaluate the contribution of the atoms produced by the dissociation around the edge and the ergodic region.

Acknowledgements

This study is supported by the collaboration program at NIFS (NIFS02KLPH001). The author would like to show grateful acknowledgement to the associated staffs at NIFS and the members of the LHD experimental group for their excellent and helpful support.

References

[1] A. Loarte et al., Nucl. Fusion 38 (1998) 331.
[2] J.L. Terry et al., Phys. Plasmas 5 (1998) 1759.
[3] U. Wenzel et al., Nucl. Fusion 39 (1999) 873.
[4] R.C. Isler et al., Phys. Plasmas 4 (1997) 2989.
[5] H. Kubo et al., J. Nucl. Mater. 337–339 (2005) 161.
[6] U. Wenzel et al., Nucl. Fusion 44 (2004) 1130.
[7] J. Miyazawa et al., Nucl. Fusion 46 (2006) 532.
[8] S. Sudo et al., Plasma Phys. Control. Fusion 45 (2003) 1127.
[9] H. Kawazome et al., J. Nucl. Mater. 313–316 (2003) 716.
[10] D. Reiter et al., J. Nucl. Mater. 196–198 (1992) 1059.
[11] J.P. Biersack et al., Appl. Phys. A 34 (1984) 73.
[12] T. Loarer et al., JET-R(99)05.
[13] H. Kubo et al., Plasma Phys. Control. Fusion 40 (1998) 1115.
[14] S. Masuzaki et al., J. Plasma Fusion Res. 81 (2005) 649.